Annals of the University of Craiova, Mathematics and Computer Science Series
Volume 49(2), 2022, Pages 250–259, DOI: 10.52846/ami.v49i2.1532
ISSN: 1223-6934

Color image completion using tensor truncated nuclear norm with l_0 total variation

Karima El Qate, Souad Mohaoui, Abdelilah Hakim, and Said Raghay

Abstract. In recent years, the problem of incomplete data has been behind the appearance of several completion methods and algorithms. The truncated nuclear norm has been known as a powerful low-rank approach both for the matrix and the tensor cases. However, the low-rank approaches are unable to characterize some additional information exhibited in data such as the smoothness or feature-preserving properties. In this work, a tensor completion model based on the convex truncated nuclear norm and the nonconvex-sparse total variation is introduced. Notably, we develop an alternating minimization algorithm that combines the accelerating proximal gradient for the convex step and a projection operator for the nonconvex step to solve the optimization problem. Experiments and comparative results show that our algorithm has a significant impact on the completion process.

2010 Mathematics Subject Classification. Primary 60J05; Secondary 60J20.
Key words and phrases. Missing values, Tensor recovery, Truncated nuclear norm, l_0 total variation, color images.

1. Introduction

Recovering missing values in multidimensional data is the main goal of tensor completion methods. Hence, the classic tensor completion problems assume the low-rankness properties of the underlying multidimensional data. Commonly, the tensor nuclear norm which is based on extending the definition of the matrix nuclear norm to the tensor case is employed to depict the low-rankness prior to data. A basic approach to completion problem is to directly minimize the tensor rank

$$\begin{aligned} &\min_{\mathcal{X}} \ \operatorname{rank}(\mathcal{X}) \\ &\text{s.t} \ \ \|\mathcal{P}_\Omega(\mathcal{X}) - \mathcal{P}_\Omega(\mathcal{M})\|_F \leq \epsilon. \end{aligned} \tag{1}$$

where $\mathcal{X} \in \mathbb{R}^{p_1 \times p_2 \times p_3}$ is the recovered tensor, $\mathcal{M}$ is the observed tensor, r is a given bound rank of low-rank $\mathcal{X}$, and $\mathcal{P}_\Omega$ denotes the projection of $\mathcal{X}$ on the observed set Ω which is defined by

$$\mathcal{P}_\Omega(\mathcal{X}) = \begin{cases} \mathcal{X}_{i_1,i_2,\ldots,i_n} & \text{if } (i_1, i_2, \ldots, i_n) \in \Omega, \\ 0 & \text{otherwise.} \end{cases}$$

The rank function is non-convex with respect to $\mathcal{X}$, and the problem (1) is NP-hard. Thus, as for the matrix case, the nuclear norm is then considered as the convex surrogate of the nonconvex rank function. The definition of the nuclear norm of a tensor is a complicated issue since it cannot be intuitively derived from the

Received August 13, 2021. Accepted January 9, 2022.

matrix case. Several versions of tensor nuclear norms have been proposed, but they are quite different from each other. A recent version of the tensor nuclear norm is the tubal nuclear norm (Tubal-NN) which stands on the new definition of tensor-tensor product and the tensor singular value decomposition (T-SVD). The Tubal-NN is defined as the sum of nuclear norms of all frontal slices in the Fourier domain. Different from the nuclear norm-based approaches which minimize the summation of all the singular values, the truncated nuclear regularization TNNR problem only minimizes the smallest $\min(p_1, p_2) - r$ singular values since the rank of a matrix only correspond to the r nonzero singular values. The truncated nuclear norm has proved to be more accurate and robust in approximating the rank function for both matrix and tensors [11, 1, 7, 3, 4].

On the other hand, exploiting spatial difference information of data becomes an efficient way to improve the tensor completion performance. Specifically, the total variation (TV) based l_1 norms that has been receiving much attention due to the smoothness property. The success of total variation-based methods for image processing is due to their ability to preserve edges in images. However, using the convex l_1-TV which penalizes the large gradient magnitudes may affect the preservation of the sharp edges. To address this drawback, a nonconvex-sparse l_0 norm-based TV regularization, furthering the sparsity in the gradient domain has been introduced in [8].

This paper takes a step in this direction by introducing a tensor completion model that combines the Nonconvex-Sparsity TV term and the tensor truncated nuclear norm. This model improved the completion performance since it imposed the l_0 norm on the spatial-spectral difference information of data, which can give rise to truly piecewise structure and better enhance highest-contrast edges by confining the number of nonzero gradients [8]. To solve the proposed model, we exploit the accelerated proximal alternating minimization framework and we design a tensor completion algorithm called truncated nuclear norm-based sparse total variation (TNNR-STV). The experimental results showed that the proposed algorithm provides better completion performances for color images comparing with different popular tensor completion algorithms.

2. Preliminaries

In this section, we introduce basic notation and definitions on tenors used through the rest of this paper. It will be convenient to break a tensor $\mathcal{X} \in \mathbb{R}^{p_1 \times p_2 \times p_3}$ up into various slices and tubal elements and to have indexing on those. Using Matlab notation, $\mathcal{X}(i, :, :)$ corresponds to the i^{th} horizontal slice, $\mathcal{X}(:, i, :)$ corresponds to the i^{th} lateral slice, and $\mathcal{X}(:, :, i)$ corresponds the i^{th} frontal slice.

fold / unfold

$$\mathbf{unfold}(\mathcal{X}) = \begin{bmatrix} X_{(1)} \\ X_{(2)} \\ \vdots \\ X_{(p_3)} \end{bmatrix}, \quad \mathbf{fold}(\mathbf{unfold}(\mathcal{X})) = \mathcal{X}.$$

Where $X_{(i)}$ refers to the i^{th} frontal slice $\mathcal{X}(:, :, i)$.

For multiplication between two tensors, we introduce the concept of converting $\mathcal{X}$

into a block circulant matrix, which is defined as

$$\mathbf{bcirc}(\mathcal{X}) = \begin{bmatrix} X_{(1)} & X_{(p_3)} & X_{(p_3-1)} & \dots & X_{(2)} \\ X_{(2)} & X_{(1)} & X_{(p_3)} & \dots & X_{(3)} \\ \vdots & \vdots & \vdots & \ddots & \vdots \\ X_{(p_3)} & X_{(p_3-1)} & X_{(p_3-2)} & \dots & X_{(1)} \end{bmatrix},$$

Let $\mathcal{X}$ be an $p_1 \times p_2 \times p_3$ tensor and F_{p_3} be the $p_3 \times p_3$ DFT matrix, then

$$(F_{p_3} \otimes I_{p_1}).\,\mathbf{bcirc}(\mathcal{X}).(F_{p_3}^* \otimes I_{p_2}) = \hat{X}.$$

where $\otimes$ denotes the Kronecker product, F^* denotes the conjugate transpose of F, and "." refers to the standard matrix product. We denote $\hat{X} \in \mathbb{R}^{p_1 p_3 \times p_2 p_3}$ as a block diagonal matrix with its i^{th} block on the diagonal as the i^{th} frontal slice $\hat{X}_{(i)}$ of $\hat{\mathcal{X}}$.

Definition 2.1 (T-product)**.** Let $\mathcal{X}_1 \in \mathbb{R}^{p_1 \times p_2 \times p_3}$ and $\mathcal{X}_2 \in \mathbb{R}^{p_2 \times p_4 \times p_3}$ be 3-way tensors. Then the tensor product (T-product) $\mathcal{X}_1 * \mathcal{X}_2$ is the $p_1 \times p_4 \times p_3$ tensor

$$\mathcal{X}_1 * \mathcal{X}_2 = \mathbf{fold}\left(\mathbf{bcirc}(\mathcal{X}_1).\,\mathbf{unfold}(\mathcal{X}_2)\right). \tag{2}$$

Definition 2.2. Let $\mathcal{X} \in \mathbb{R}^{p_1 \times p_2 \times p_3}$ be a given tensor. Its conjugate transpose denoted by $\mathcal{X}^T \in \mathbb{R}^{p_2 \times p_1 \times p_3}$ is obtained by conjugate transposing each frontal slice and then reversing the order of transposed frontal slices 2 through p_3

$$\mathcal{X}^T = \mathbf{fold}\left([{X^{(1)}}^T, {X^{(p_3)}}^T, \dots, {X^{(3)}}^T, {X^{(2)}}^T]\right)^T.$$

Definition 2.3. The tensor $\mathcal{Q}$ is orthogonal in the sense of the T-product if

$$\mathcal{Q} * \mathcal{Q}^T = \mathcal{Q}^T * \mathcal{Q} = \mathcal{I}.$$

We define the tensor singular values decomposition denoted by T-SVD.

Definition 2.4 (Tensor singular value decomposition)**.** Let $\mathcal{X}$ be an $p_1 \times p_2 \times p_3$ real valued tensor, the T-SVD is defined as

$$\mathcal{X} = \mathcal{U} * \mathcal{S} * \mathcal{V}^T, \tag{3}$$

where $\mathcal{U}$ and $\mathcal{V}$ are orthogonal $p_1 \times p_1 \times p_3$ and $p_2 \times p_2 \times p_3$, respectively, and $\mathcal{S}$ is a $p_1 \times p_2 \times p_3$ f-diagonal tensor.

We consider the Discrete Fourier Transformation (DFT) on tensors. For a tensor $\mathcal{X}$, we denote $\hat{\mathcal{X}}$ as the result of DFT on $\mathcal{X}$ along the 3^{rd} dimension, i.e., performing the DFT on all the tubes of $\mathcal{X}$. By using the Matlab command fft, we have $\hat{\mathcal{X}} = \text{fft}(\mathcal{X}, [\,], 3)$. In a similar way, we can compute $\mathcal{X}$ from $\hat{\mathcal{X}}$ using the inverse FFT, i.e., $\mathcal{X} = \text{ifft}(\hat{\mathcal{X}}, [\,], 3)$.

Definition 2.5 (Truncated nuclear norm)**.** Given a tensor $\mathcal{X} \in \mathbb{R}^{p_1 \times p_2 \times p_3}$, the tensor nuclear norm $\|\mathcal{X}\|_r$ is defined as the sum of $\min(p_1, p_2) - r$ minimum singular values

$$\|\mathcal{X}\|_r = \sum_{i=r+1}^{\min(p_1,p_2)} \sigma_i(\mathcal{X}). \tag{4}$$

The tensor truncated nuclear norm (4) can be reformulated as follows [1]

$$\begin{aligned}\|\mathcal{X}\|_r &= \|\hat{X}_{(1)}\|_r = \sum_{i=r+1}^{\min(p_1,p_2)} \sigma_i(\hat{X}_{(1)}) = \|\hat{X}_{(1)}\|_* - \sum_{i=1}^{r} \sigma_i(\hat{X}_{(1)}),\\ &= \|\hat{X}_{(1)}\|_* - \max_{\substack{\hat{A}_{(1)}\hat{A}_{(1)}^T=I\\ \hat{Q}_{(1)}\hat{Q}_{(1)}^T=I}} \operatorname{tr}(\hat{A}_{(1)}\hat{X}_{(1)}\hat{Q}_{(1)}^T),\\ &= \|\mathcal{X}\|_* - \max_{\substack{\mathcal{A}*\mathcal{A}^T=\mathcal{I}\\ \mathcal{Q}*\mathcal{Q}^T=\mathcal{I}}} \operatorname{tr}(\mathcal{A}*\mathcal{X}*\mathcal{Q}^T).\end{aligned}$$

where $\mathcal{A}$ and $\mathcal{B}$ are generated from the t-SVD of $\mathcal{X}$ by (13).

Definition 2.6 (Mixed $l_{1,0}$ pseudo-norm)**.** For a given vector $\mathbf{y} \in \mathbb{R}^m$ and index sets $s_1, \ldots, s_i, \ldots, s_n (1 \le n \le m)$ that satisfies the following properties

- Each s_i is a subset of $1, \ldots, \mathrm{m}$,
- $s_i \cap s_l = \emptyset$ for any $i \neq l$
- $\cup_{i=1}^{n} s_i = 1, \ldots, m$

the mixed $l_{1,0}$ pseudo-norm of y is defined as:

$$\|\mathbf{y}\|_{1,0}^s = \|(\|\mathbf{y}_{s_1}\|_1, \ldots, \|\mathbf{y}_{s_i}\|_1, \ldots \|\mathbf{y}_{s_n}\|_1)\|_0 \tag{5}$$

where $\mathbf{y}_{s_i}$ denotes a sub-vector of $\mathbf{y}$ with its entries specified by s_i and $\|\cdot\|_0$ calculates the number of the non-zero entries in $(\cdot)$.

Definition 2.7 (Indicator function)**.** Let $\mathcal{B}$ be a given operator and γ be a positive fixed integer, the indicator function of $l_{1,0}$ mixed pseudonorm is defined as follows

$$I_{\|\mathcal{B}\cdot\|_{1,0}^s}(y) = \begin{cases} 0, & \|\mathcal{B}\mathbf{y}\|_{1,0}^s \le \gamma \\ \infty, & \text{otherwise} \end{cases} \tag{6}$$

3. Main results

We introduce a low-rank tensor completion model based on the TNNR. Beside, a nonconvex-sparsity TV regularization term is included to enhance important components in a given current data. Now, before introducing the new tensor completion model based on the l_0 TV term and TNNR term, we first brief review the l_0 TV model.

3.1. From Matrix l_0-gradient to the tensor l_0-TV model. The l_0 gradient penalty has become a powerful tool for edge-preserving property by globally controlling the number of nonzero gradients [8]. The l_0 gradient of a matrix data $\mathbf{Z} \in \mathbb{R}^{h,v}$ is defined by:

$$\begin{aligned} l_0\mathrm{TV}(\mathbf{Z}) &= \sum C\left(\|D_1\mathbf{Z}\|_1 + \|D_2\mathbf{Z}\|_1\right)\\ &= \sum_{i}^{h}\sum_{j}^{v} C\left(|\mathbf{Z}_{i+1,j} - \mathbf{Z}_{i,j}| + |\mathbf{Z}_{i,j+1} - \mathbf{Z}_{i,j}|\right)\end{aligned} \tag{7}$$

where D_1 and D_2 are the difference operators along the first and second directions of the image. $C(\mathbf{Z})$ is a binary function that count the number of non-zeros gradients

and witch verify

$$C(\mathbf{Z}) := \begin{cases} 1, & \text{if } \mathbf{Z} \neq 0 \\ 0, & \text{otherwise} \end{cases} \tag{8}$$

Now, by extending this definition of l_0 gradient to the tensorial framework, the definition become for a given third order tensor $\mathcal{Z} \in \mathbb{R}^{h,v,b}$ as follow

$$l_0\text{TV}(\mathcal{Z}) = \sum_{i}^{h}\sum_{j}^{v} C\left(\sum_{k}^{b}\left(|\mathcal{Z}_{i+1,j,k} - \mathcal{Z}_{i,j,k}| + |\mathcal{Z}_{i,j+1,k} - \mathcal{Z}_{i,j,k}|\right)\right) \tag{9}$$

where boundary values of gradients are defined as follows

$$\begin{cases} \mathcal{Z}_{i,j+1,k} - \mathcal{Z}_{i,j,k} = 0, & \text{if} \quad i = h \\ \mathcal{Z}_{i+1,j,k} - \mathcal{Z}_{i,j,k} = 0, & \text{if} \quad j = v \end{cases} \tag{10}$$

Here, the $l_0\text{TV}(\mathcal{X})$ counts the non-zeros of spatial difference information with the assistance of third-mode information. Using definition 2.6, another formulation of the l_0-TV becomes:

$$l_0\text{TV}(\mathcal{Z}) = \|\mathcal{B}D\mathcal{Z}\|_{1,0}^{s} \tag{11}$$

where operator D is an operator to calculate both first-mode and second-mode differences. The given operator $\mathcal{B}$ forces boundary values of gradients to be zero when $i = h$ and $j = v$.

3.2. Tensor completion via TNNR with nonconvex-sparse TV prior. Given a tensor $\mathcal{X} \in \mathbb{R}^{p_1 \times p_2 \times p_3}$, the truncated nuclear norm $\|\mathcal{X}\|_r$ completion problem is formulated as:

$$\begin{gathered} \min_{\mathcal{X}} \|\mathcal{X}\|_* - \max_{\substack{\mathcal{A}*\mathcal{A}^T=\mathcal{I} \\ \mathcal{Q}*\mathcal{Q}^T=\mathcal{I}}} \text{tr}(\mathcal{A} * \mathcal{X} * \mathcal{Q}^T) \\ \text{s.t} \quad \|\mathcal{P}_\Omega(\mathcal{X} - \mathcal{M})\|_F \leq \epsilon. \end{gathered} \tag{12}$$

where $\mathcal{A}$ and $\mathcal{Q}$ are updated at each iteration using the tensor singular values decomposition of the computed tensor $\mathcal{X}$. We define the operator of selecting the first r columns in the second dimension of $\mathcal{U}$ and $\mathcal{V}$, with Matlab notation, used also for updating $\mathcal{A}$ and $\mathcal{Q}$ at each iteration

$$\mathcal{A} = \mathcal{U}(:, 1:r, :)^T, \quad \mathcal{Q} = \mathcal{V}(:, 1:r, :)^T. \tag{13}$$

The tensor $\mathcal{X}$ can be updated by minimizing the objective function

$$\begin{gathered} \min_{\mathcal{X}} \|\mathcal{X}\|_* - \text{tr}(\mathcal{A} * \mathcal{X} * \mathcal{Q}^T) \\ \text{s.t} \quad \|\mathcal{P}_\Omega(\mathcal{X} - \mathcal{M})\|_F \leq \epsilon. \end{gathered} \tag{14}$$

The proposed nonconvex-sparse tensor completion formulation can be expressed by the following optimization problem:

$$\begin{gathered} \min_{\mathcal{X}} \frac{\mu}{2} \|\mathcal{P}_\Omega(\mathcal{X}) - \mathcal{P}_\Omega(\mathcal{M})\|_F^2 - \text{tr}\left(\mathcal{A} * \mathcal{X} * \mathcal{Q}^T\right) + \|\mathcal{X}\|_* \\ \text{s.t.} \ \|BD\mathcal{X}\|_{1,0}^{s} \leq \gamma \end{gathered} \tag{15}$$

First, we introduce an auxiliary variable $\mathcal{W}$ to relax the model. For this purpose, we first rewrite (15) to be the following equivalent problem:

$$\begin{gathered} \min_{\mathcal{W},\mathcal{X}} \frac{\mu}{2} \|\mathcal{P}_\Omega(\mathcal{X}) - \mathcal{P}_\Omega(\mathcal{M})\|_F^2 - \text{tr}\left(\mathcal{A} * \mathcal{X} * \mathcal{Q}^T\right) + \|\mathcal{X}\|_* + I_{\|\mathcal{B}\cdot\|_{1,0}^{s}}(\mathcal{W}) \\ \text{s.t.} \quad \mathcal{W} = D\mathcal{X} \end{gathered} \tag{16}$$

which is equivalent to the following basic problem

$$\min_{\mathcal{W},\mathcal{X}} \ \frac{\mu}{2}\|\mathcal{P}_\Omega(\mathcal{X})-\mathcal{P}_\Omega(\mathcal{M})\|_F^2-\text{tr}\left(\mathcal{A}*\mathcal{X}*\mathcal{Q}^T\right)+\frac{\rho}{2}\|\mathcal{W}-D\mathcal{X}\|_F^2+\|\mathcal{X}\|_*+I_{\|\mathcal{B}\cdot\|_{1,0}^s}(\mathcal{W}) \tag{17}$$

To solve the aforementioned problem, we propose an alternating method based on an accelerated proximal gradient [5] step and a projection step. The accelerated proximal gradient algorithm alternatively applies the proximal gradient method to each subproblem. Differently, in the proposed algorithm we use the proximal gradient method for the computation of $\mathcal{X}_k$-subproblem while we consider the projection onto $l_{1,0}$ to calculate the auxiliary variable at the current iterate $\mathcal{W}_k$. The use of the acceleration technique can be explained as follows. If the current iterate $\mathcal{X}_k$ approaches the optimal point $\mathcal{X}^*$ more than the previous iterate $\mathcal{X}_{k+1}$, then the extrapolation point may be closer to $\mathcal{X}^*$ than $\mathcal{X}_k$ with appropriate extrapolation weight.

The objective function is the sum of a smooth and convex functions. Thus, let f be the smooth function defined as follows

$$f(\mathcal{X},\mathcal{W}) \ = \ \frac{\mu}{2}\|\mathcal{P}_\Omega(\mathcal{X})-\mathcal{P}_\Omega(\mathcal{M})\|_F^2-\text{tr}\left(\mathcal{A}*\mathcal{X}*\mathcal{Q}^T\right)+\frac{\rho}{2}\|\mathcal{W}^k-D\mathcal{X}\|_F^2 \tag{18}$$

The proposed accelerated alternating method consists of the following steps:

$$\begin{cases} t_k=\frac{1+\sqrt{4t_{k-1}^2+1}}{2} \\ w_k=\frac{t_{k-1}-1}{t_k} \\ \mathcal{Y}_k=\mathcal{X}_k+w_k\left(\mathcal{X}_k-\mathcal{X}_{k-1}\right) \\ \mathcal{X}_{k+1}=\text{Prox}_{\tilde{\rho}}^{\|\cdot\|_*}\left(\mathcal{Y}_k-\tilde{\rho}^{-1}\nabla_{\mathcal{Y}_k}f\left(\mathcal{Y}_k,\mathcal{W}_k\right)\right) \\ \mathcal{W}_{k+1}=\arg\min_{\mathcal{W}} \ f(\mathcal{X}_{k+1},\mathcal{W})+I_{\|\mathcal{B}\cdot\|_{1,0}^s}(\mathcal{W}) \end{cases} \tag{19}$$

with initial value $t_0=1$, $\nabla_{\mathcal{X}}f(\mathcal{X},\mathcal{W}) \ = \ \mu(\mathcal{P}_\Omega(\mathcal{X})-\mathcal{P}_\Omega(\mathcal{Y}))-\mathcal{A}_k^T*\mathcal{Q}_k+\rho D^T(\mathcal{W}_k-D\mathcal{X})$ and the proximal mapping is defined as

$$\text{Prox}_\rho^{\|\cdot\|_*}(\mathcal{X}) \ = \ \arg\min_{\mathcal{X}} \ \frac{1}{2}\|\mathcal{X}-\mathcal{Y}\|_F^2+\frac{1}{\rho}\|\mathcal{X}\|_*.$$

The proximal operator of the nuclear norm regularization is given by the singular value thresholding operator, denoted by $\mathcal{D}_{\frac{1}{\rho}}(\mathcal{X})$

$$\mathcal{D}_{\frac{1}{\rho}}(\mathcal{X}) \ = \ \mathcal{U}*\mathcal{S}_{\frac{1}{\rho}}(\mathcal{S})*\mathcal{V}^T. \tag{20}$$

where $\mathcal{S}_\tau$ is the soft-thresholding operator. In the tensorial case, the thresholding is applied on each frontal slice of the given tensor $\mathcal{X}\in\mathbb{R}^{p_1\times p_2\times p_3}$

$$\mathcal{S}_\tau(\mathcal{X}) \ = \ \text{ifft}(\mathcal{S}_\tau(\hat{\mathcal{X}})), \tag{21}$$

where

$$\mathcal{S}_\tau(\hat{X}_{(i)}) \ = \ \text{diag}(\max\{\sigma_i-\tau,0\}_{1\le i\le r}), \quad i=1,2,...,p_3. \tag{22}$$

Now, for the sub-problem of $\mathcal{W}_{k+1}$ can be expressed by the following constrained minimization problem:

$$\begin{aligned} \min_{\mathcal{W}} \ & \|\mathcal{W}-\mathcal{X}_{k+1}\|_F^2 \\ \text{s.t.} \quad & \|B\mathcal{W}\|_{1,0}^s\le\gamma \end{aligned} \tag{23}$$

The resolution of problem (23) is performed by the following Proposition.

Proposition 3.1 (Projection onto $l_{1,0}$ mixed pseudo-norm ball with binary mask [6])**.** *Set $\mathbf{y} \in \mathbb{R}^m$ as a known vector, set γ as a non-negative integer. Let $\mathbf{W}$ be a known diagonal binary matrix, and let $s_1, \ldots, s_i, \ldots, s_n (1 \leq n \leq m)$ be index sets satisfying the conditions from definition 2.6. Without loss of generality, $\mathbf{W}\mathbf{y} = \left(\mathbf{y}_{s_1}^T \ldots \mathbf{y}_{s_n}^T\right)^T$ are assumed. $\mathbf{y}_{s_1} \ldots \mathbf{y}_{s_n}$ are sorted in descending order according to $\left\|\mathbf{y}_{s_{\vec{1}}}\right\|_2 > \left\|\mathbf{y}_{s_{\vec{2}}}\right\|_2 > \ldots > \left\|\mathbf{y}_{s_{\vec{n}}}\right\|_2$, where $\mathbf{y}_{s_{\vec{1}}} \ldots \mathbf{y}_{s_{\vec{n}}}$ are obtained with the new order, and the original index sets i have $\vec{i}$ that corresponds to it one by one. For the following problem*

$$\mathbf{z}^\star \in \underset{\mathbf{z}\in\mathbb{R}^m}{\operatorname{argmin}} \|\mathbf{y} - \mathbf{z}\|^2 \quad t.q \quad \|W\mathbf{z}\|_{1,0}^s \leq \alpha$$

one of the optimal solution is given by:

$$\mathbf{z}^\star = \begin{cases} \mathbf{y}, & \text{if} \quad \|\mathbf{W}\mathbf{y}\|_{1,0}^s \leq \alpha, \\ \left(\overline{\mathbf{y}}_{s_{\vec{1}}}^\top \cdots \overline{\mathbf{y}}_{s_{\vec{n}}}^\top\right)^\top + (\mathbf{I} - \mathbf{W})\mathbf{y}, & \text{if} \quad \|\mathbf{W}\mathbf{y}\|_{1,0}^s > \alpha, \end{cases}$$

where,

$$\overline{\mathbf{y}}_{s_{\vec{k}}}^\top := \begin{cases} \mathbf{y}_{s_k}^\top, & \text{if} \quad k \in \{(1), \ldots, (\alpha)\}, \\ \mathbf{0}, & \text{if} \quad k \in \{(\alpha+1), \ldots, (n)\} \end{cases}$$

4. Numerical results

This section presents the numerical results in which we evaluate the performance of the proposed TNNR-STV completion algorithm. We conduct experiments on four benchmark 3D channel RGB color images. The missing values are distributed randomly. The accuracy of the obtained results are measured by the peak signal to noise ratio (PSNR) and structural similarity (SSIM).

We present in Table 1, the PSNR and SSIM values of the obtained results of different tests using the three images with different choices of the percentage of missing data. The best value of the PSNR is the number written in italics on each row. Overall, we clearly observe that the proposed TNNR-STV model presents larger PSNR and SSIM values compared with the three tensor completion methods which assures the efficiency of our algorithm.

To further show the significant impact of our algorithm on the completion of RGB color images, we visually compare the results of the four tensor completion methods. Thus, in Figures 1, 2, and Figure 3 we show the simulated images compared with the recovered images using T-TNN, LRTC, MF_TV and our proposed TNNR-STV model for test images with 70% of missing values respectively. Visually, we can ensure that our approach reconstruct the missing pixels effectively.

5. Conclusion

In this paper, we consider the color image completion problem by introducing a model-based nonconvex regularization. Besides, we have integrated the truncated nuclear norm schema for exhibiting the low-rankness representation. The main idea is to enforce the l_0 norm on the spatial difference images without ignoring the spectral

TABLE 1. The PSNR/SSIM obtained by the completion of four images with the percentage of missing entries 90%, 80%, 70%, and 60%. For each test, the results of LRTC [10], T-TNN [9], MF-TV [2], and our proposed TNNR-STV are illustrated and the best among the results is highlight in bold face.

SR	90%		80%		70%		60%	
Methods	PSNR	SSIM	PSNR	SSIM	PSNR	SSIM	PSNR	SSIM
				Plat				
T-TNN	20.91	0.3568	23.98	0.5446	26.18	0.6643	28.06	0.7601
LRTC	20.22	0.3129	23.56	0.4951	25.85	0.6242	27.66	0.7229
MF-TV	16.96	0.2636	19.28	0.3246	23.92	0.5107	**29.33**	0.7563
TNNR-STV	**21.29**	**0.3701**	**24.13**	**0.5572**	**26.18**	**0.6722**	28.26	**0.7564**
				House				
T-TNN	20.34	0.3817	24.81	0.6241	27.92	0.7538	30.32	0.8295
LRTC	19.77	0.3533	24.54	0.6037	27.61	0.7380	30.10	0.8208
MF-TV	9.378	0.0496	17.68	0.3116	26.68	0.7640	28.33	0.8553
TNNR-STV	**20.59**	**0.4112**	**25.18**	**0.6142**	**28.12**	**0.7651**	**30.63**	**0.8297**
				Parthenon				
T-TNN	18.78	0.3874	22.81	0.6289	25.71	0.7616	28.43	0.8521
LRTC	18.39	0.3689	22.60	0.6180	25.47	0.7520	28.56	0.8472
MF-TV	8.259	0.0608	13.76	0.2140	20.86	0.5117	28.75	0.8264
TNNR-STV	**19.86**	**0.4241**	**23.30**	**0.6377**	**26.16**	**0.7734**	**28.75**	**0.8608**

information. The proposed algorithm has been shown to be effective for recovering the missing values in color images.

References

[1] Y. Hu, D. Zhang, J. Ye, X. Li, and X. He, Fast and accurate matrix completion via truncated nuclear norm regularization, *IEEE transactions on pattern analysis and machine intelligence* **35** 9 (2012), no. 9, 2117–2130. DOI: 10.1109/TPAMI.2012.271

[2] T.-Y. Ji, T.-Z. Huang, X.-L. Zhao, T.-H. Ma, and G. Liu, Tensor completion using total variation and low-rank matrix factorization, *Information Sciences* **326** (2016), 243–257. DOI: 10.1016/j.ins.2015.07.049

[3] Q. Liu, Z. Lai, Z. Zhou, F. Kuang, and Z. Jin, A truncated nuclear norm regularization method based on weighted residual error for matrix completion, *IEEE Transactions on Image Processing* **25** (2015), no. 1, 316–330. DOI: 10.1109/TIP.2015.2503238

[4] S. Mohaoui, A. Hakim, and S. Raghay, Tensor completion via bilevel minimization with fixed-point constraint to estimate missing elements in noisy data, *Advances in Computational Mathematics* **47** (2021), no. 1, 1–27. DOI: 10.1007/s10444-020-09841-8

[5] Y. Nesterov, Gradient methods for minimizing composite functions, *Mathematical Programming* **140** (2013), no. 1, 125–161. DOI: 10.1007/s10107-012-0629-5

[6] S. Ono, $L_{\{}0\}$ gradient projection, *IEEE Transactions on Image Processing* **26** (2017), no. 4, 1554–1564. DOI: 10.1109/TIP.2017.2651392

[7] Y. Song, J. Li, X. Chen, D. Zhang, Q. Tang, and K. Yang, An efficient tensor completion method via truncated nuclear norm, *Journal of Visual Communication and Image Representation* **70** (2020), 102791. DOI: 10.1016/j.jvcir.2020.102791

FIGURE 1. The visual comparison results of the recovered *House* image. From left to right and to bottom, the original image, the incomplete image with 30% of observation, the recovered results by T-TNN, LRTC, MF_TV, and the proposed NC_TV respectively.

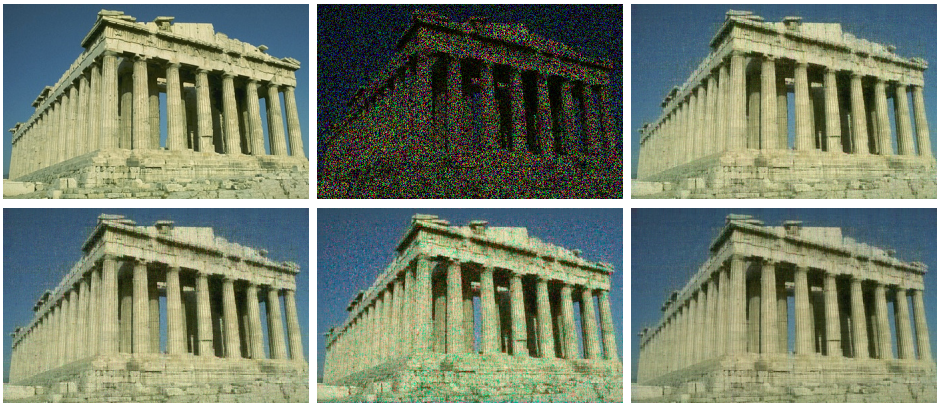

FIGURE 2. The visual comparison results of the recovered *Plat* image. The original image, the incomplete image with 30% of observation,the recovered results by T-TNN, LRTC, MFTV, and the proposed TNNR-STV respectively.

[8] M. Wang, Q. Wang, and J. Chanussot, Tensor low-rank constraint and l_0 total variation for hyperspectral image mixed noise removal, *IEEE Journal of Selected Topics in Signal Processing* **15** (2021), no. 3, 718–733. DOI: 10.1109/JSTSP.2021.3058503

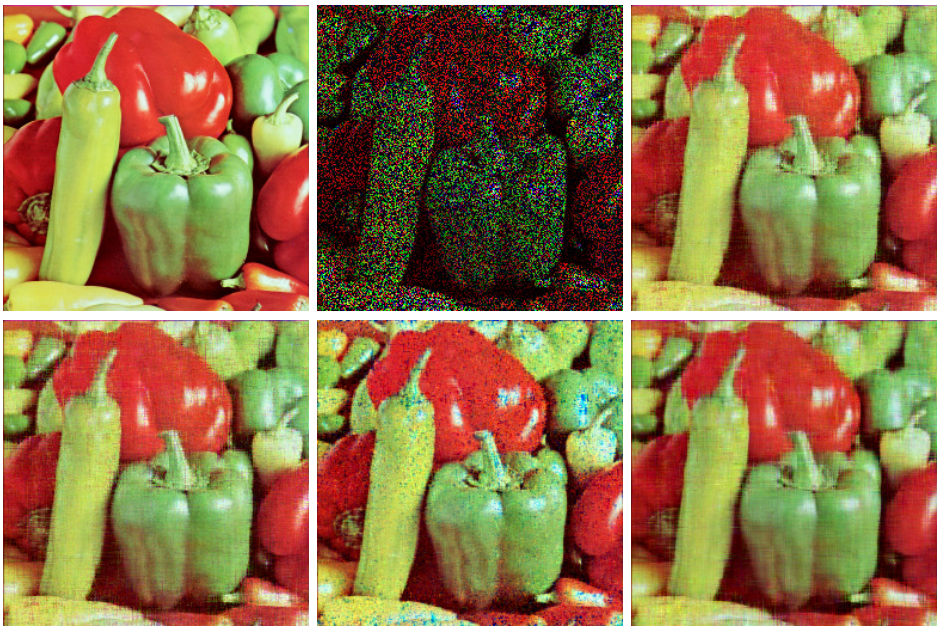

FIGURE 3. The visual comparison results of the recovered *Peppers* image. The original image, the incomplete image with 30% of observation, the recovered results by T-TNN, LRTC, MF_TV, and the proposed TNNR-STV respectively.

[9] J. Wright, A. Ganesh, S. Rao, and Y. Ma, Robust principal component analysis: Exact recovery of corrupted low-rank matrices via convex optimization, Coordinated Science Laboratory Report no. UILU-ENG-09-2210, DC-243 (2009).

[10] S. Xue, W. Qiu, F. Liu, and X. Jin, Low-rank tensor completion by truncated nuclear norm regularization, In: *2018 24th International Conference on Pattern Recognition(ICPR)*, IEEE, 2600–2605, (2018).

[11] D. Zhang, Y. Hu, J. Ye, X. Li, and X. He, Matrix completion by truncated nuclear norm regularization, In: *2012 IEEE Conference on computer vision and pattern recognition*, IEEE, 2192–2199, (2012).

(Karima El Qate, Souad Mohaoui) CADI AYYAD UNIVERSITY FACULTY OF SCIENCE AND TECHNICS GUILIZ, MARRAKESH
E-mail address: karima.elqate@gmail.com, souad.mohaoui@gmail.com

(Abdelilah Hakim, Said Raghay) CADI AYYAD UNIVERSITY FACULTY OF SCIENCE AND TECHNICS GUILIZ, MARRAKESH
E-mail address: abdelilah.hakim@gmail.com, s.raghay@uca.ma